Supplement to: Sensitivities of Amazonian clouds to aerosols and updraft speed

By Micael A. Cecchini[1], Luiz A. T. Machado[1], Meinrat O. Andreae[2,12], Scot T. Martin[3], Rachel I. Albrecht[4], Paulo Artaxo[5], Henrique M. J. Barbosa[5], Stephan Borrmann[2,6], Daniel Fütterer[7], Tina Jurkat[7], Christoph Mahnke[2,6], Andreas Minikin[8], Sergej Molleker[6], Mira L. Pöhlker[2], Ulrich Pöschl[2], Daniel Rosenfeld[9], Christiane Voigt[6,7], Bernadett Weinzierl[7,10], Manfred Wendisch[11]

[1]Centro de Previsão de Tempo e Estudos Climáticos, Instituto Nacional de Pesquisas Espaciais, Cachoeira Paulista, Brasil.
[2]Biogeochemistry, Multiphase Chemistry, and Particle Chemistry Departments, Max Planck Institute for Chemistry, P.O. Box 3060, 55020, Mainz, Germany.
[3]School of Engineering and Applied Sciences and Department of Earth and Planetary Sciences, Harvard University, Cambridge, Massachusetts, USA.
[4]Departamento de Ciências Atmosféricas, Instituto de Astronomia, Geofísica e Ciências Atmosféricas (IAG), Universidade de São Paulo (USP), Brasil.
[5]Instituto de Física (IF), Universidade de São Paulo (USP), São Paulo, Brasil.
[6]Institut für Physik der Atmosphäre (IPA), Johannes Gutenberg-Universität, Mainz, Deutschland.
[7]Institut für Physik der Atmosphäre, Deutsches Zentrum für Luft- und Raumfahrt (DLR), Oberpfaffenhofen, 82234 Wessling, Deutschland.
[8]Flugexperimente, Deutsches Zentrum für Luft- und Raumfahrt (DLR), Oberpfaffenhofen, Deutschland.
[9]Institute of Earth Sciences, The Hebrew University of Jerusalem, Israel.
[10]Faculty of Physics, University of Vienna, Boltzmanngasse 5, 1090 Wien, Austria.
[11]Leipziger Institut für Meteorologie (LIM), Universität Leipzig, Stephanstr. 3, 04103 Leipzig, Deutschland.
[12] Scripps Institution of Oceanography. University of California San Diego, La Jolla, CA92093, USA.

Correspondence to: M. A. Cecchini (micael.cecchini@cptec.inpe.br)

DSD profiles for each flight

Figures S1-4 show the individual DSD profiles for each flight considered in this study. It clearly shows the cohesiveness of the aerosol effect on the vertical structure of the warm-phase. Altitudes shown are relative to cloud base.

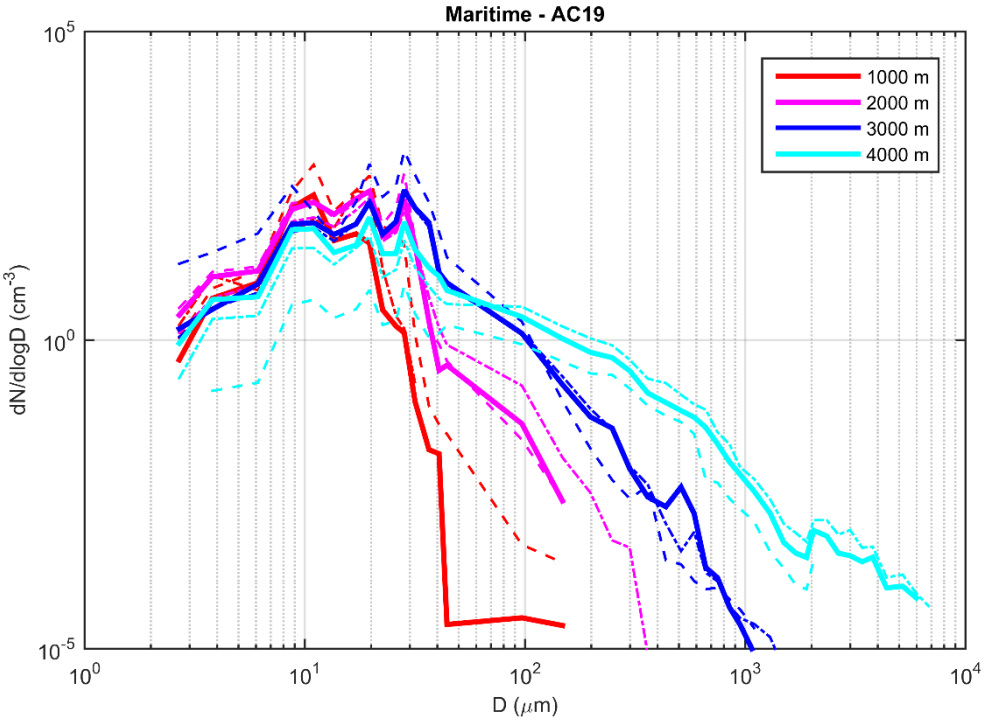

Figure S1. Droplet size distributions as function of altitude above cloud base, aerosol particle number concentration, and vertical wind speed, *W*, for flight AC19. Four 1000-m-thick layers are considered in the vertical, where the legends in the graphs show the respective upper limit of each one. Solid lines represent averaged DSDs for -1 m $s^{-1} \leq W \leq 1$ m s^{-1}, i.e., for relatively neutral vertical movements. Dashed lines represent averaged DSDs for the updraft regions where $W > 1$ m s^{-1}, and dot-dashed lines represent the downdrafts ($W < -1$ m s^{-1}).

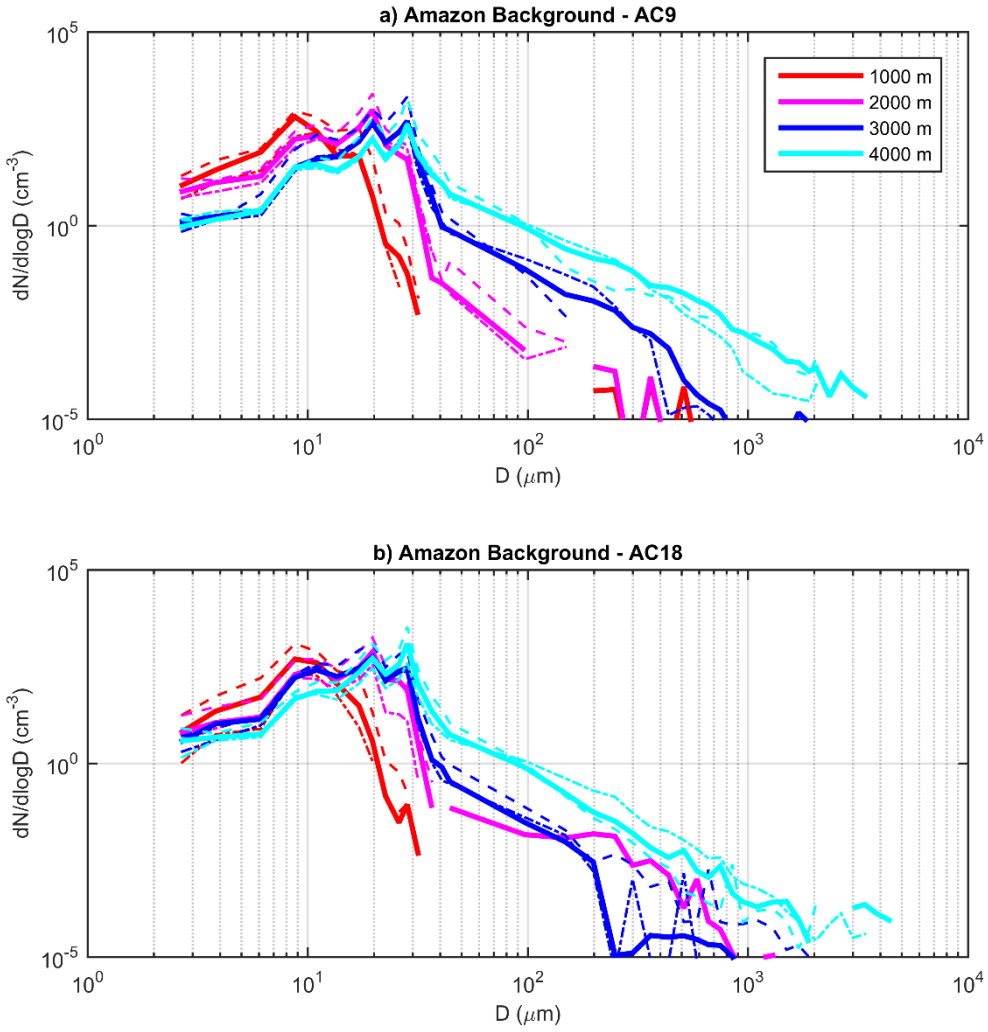

Figure S2. Droplet size distributions as function of altitude above cloud base, aerosol particle number concentration, and vertical wind speed, *W*, for flights a) AC9 and b) AC18. Four 1000-m-thick layers are considered in the vertical, where the legends in the graphs show the respective upper limit of each one. Solid lines represent averaged DSDs for -1 m $s^{-1} \leq W \leq 1$ m s^{-1}, i.e., for relatively neutral vertical movements. Dashed lines represent averaged DSDs for the updraft regions where $W > 1$ m s^{-1}, and dot-dashed lines represent the downdrafts ($W < -1$ m s^{-1}).

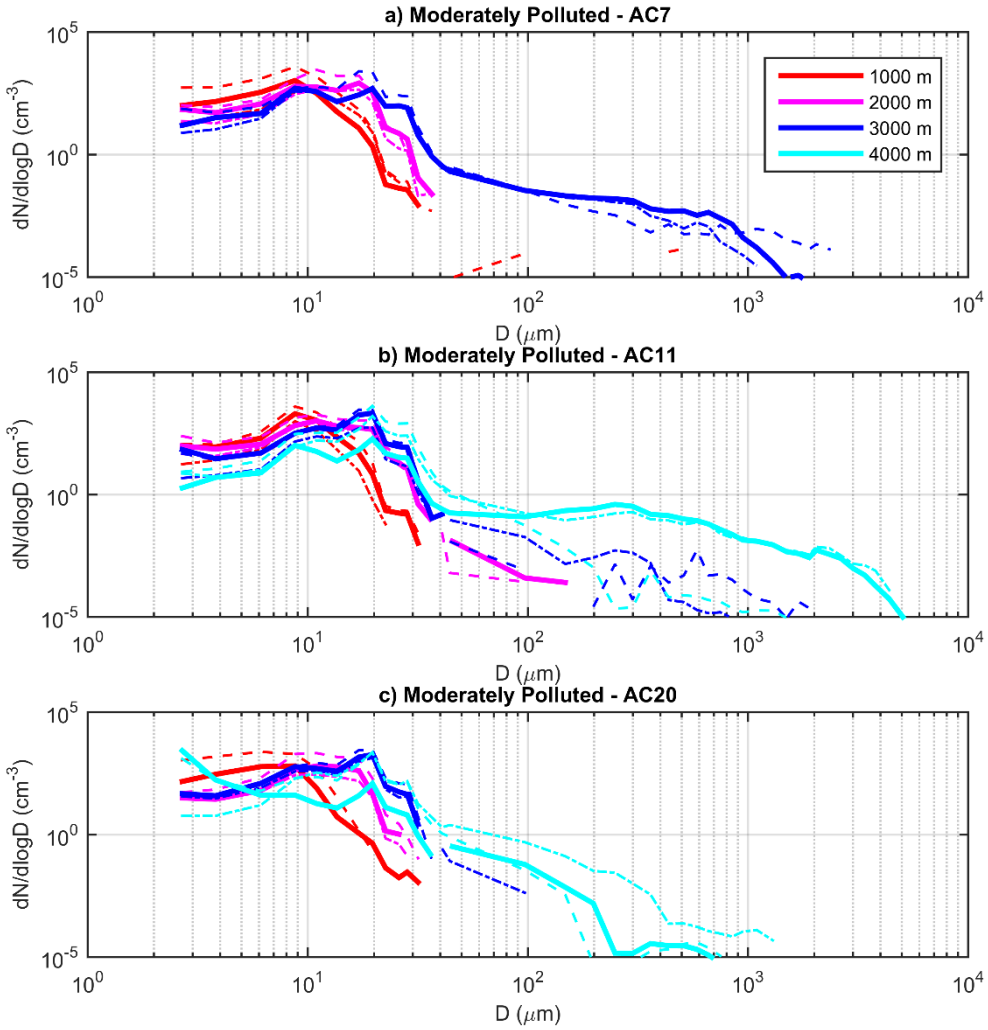

Figure S3. Droplet size distributions as function of altitude above cloud base, aerosol particle number concentration, and vertical wind speed, *W*, for flights a) AC7, b) AC11, and c) AC20. Four 1000-m-thick layers are considered in the vertical, where the legends in the graphs show the respective upper limit of each one. Solid lines represent averaged DSDs for -1 m s^{-1} ≤ W ≤ 1 m s^{-1}, i.e., for relatively neutral vertical movements. Dashed lines represent averaged DSDs for the updraft regions where W > 1 m s^{-1}, and dot-dashed lines represent the downdrafts (W < -1 m s^{-1}).

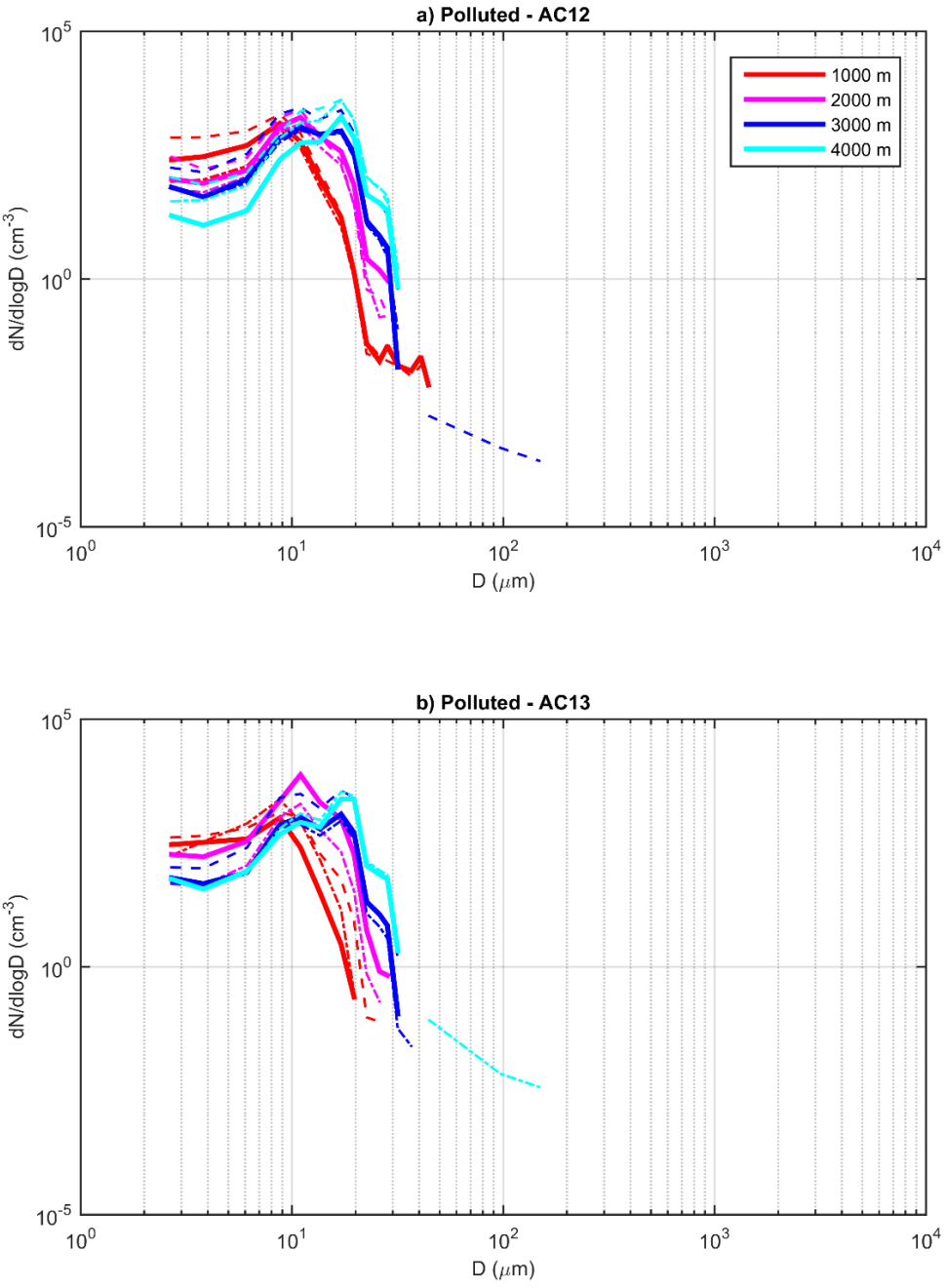

Figure S4. Droplet size distributions as function of altitude above cloud base, aerosol particle number concentration, and vertical wind speed, W, for flights a) AC12 and b) AC13. Four 1000-m-thick layers are considered in the vertical, where the legends in the graphs show the respective upper limit of each one. Solid lines represent averaged DSDs for -1 m $s^{-1} \leq W \leq 1$ m s^{-1}, i.e., for relatively neutral vertical movements. Dashed lines represent averaged DSDs for the updraft regions where $W > 1$ m s^{-1}, and dot-dashed lines represent the downdrafts ($W < -1$ m s^{-1}).

Sensitivities for individual intervals

By fixing two dimensions in the 3D matrices and varying the third, we can obtain individual sensitivities in the form of the Equation 1 in the manuscript. As an example, we can fix both *w* and *H* and obtain the sensitivities of DSD parameters to varying N_a. By using the natural logarithm scale and applying a linear fit, we obtain the sensitivity as the angular coefficient and the R^2 parameter is a measure of the significance of the relation. By calculating every possible combination, we obtain Tables S1-15 shown below. The amount of 1 Hz data for each sensitivity are shown in Tables S16-18.

w (m s^{-1}) \ H (m)	**200**	**500**	**950**	**1625**	**2637.5**	**4156.25**
0.5	-0.11 R^2 = 0.85	-0.27 R^2 = 0.96	-0.25 R^2 = 0.99	-0.23 R^2 = 0.94	-0.38 R^2 = 0.97	-0.47 R^2 = 0.71
1	-0.13 R^2 = 0.84	-0.26 R^2 = 0.93	-0.30 R^2 = 0.99	-0.18 R^2 = 0.86	-0.25 R^2 = 1.00	-0.26 R^2 = 0.96
2	-0.16 R^2 = 0.79	-0.26 R^2 = 0.98	-0.28 R^2 = 0.91	-0.17 R^2 = 0.64	-0.31 R^2 = 0.98	-0.16 R^2 = 0.53
4	-0.18 R^2 = 0.82	-0.28 R^2 = 0.95	-0.25 R^2 = 0.96	-0.25 R^2 = 0.95	-0.31 R^2 = 0.95	-0.28 R^2 = 0.99
8	-	-	-	-	-0.26 R^2 = 0.80	-0.33 R^2 = 0.98

Table S1. sensitivities of D_{eff} to N_a - $S_{D_{eff}}(N_a) = \frac{\partial lnD_{eff}}{\partial lnN_a}\Big|_{w,H}$. Intervals upper limits are highlighted in bold letters.

N_a (cm^{-3}) \ H (m)	**200**	**500**	**950**	**1625**	**2637.5**	**4156.25**
500	0.020 R^2 = 0.63	0.049 R^2 = 0.61	0.048 R^2 = 0.90	-0.018 R^2 = 0.034	0.032 R^2 = 0.77	-
1000	0.018 R^2 = 0.17	0.031 R^2 = 0.57	0.0072 R^2 = 0.029	0.046 R^2 = 0.71	0.0032 R^2 = 0.0040	0.0034 R^2 = 0.0010
3000	0.031 R^2 = 0.90	0.044 R^2 = 0.69	-	-0.011 R^2 = 0.055	0.13 R^2 = 0.93	0.18 R^2 = 0.72
4500	-0.085 R^2 = 0.97	0.013 R^2 = 0.57	0.046 R^2 = 0.62	-0.0063 R^2 = 0.23	0.021 R^2 = 0.44	0.024 R^2 = 0.48

Table S2. sensitivities of D_{eff} to w - $\boldsymbol{S_{D_{eff}}(w) = \frac{\partial lnD_{eff}}{\partial lnw}\Big|_{N_a,H}}$. Intervals upper limits are highlighted in bold letters.

N_a (cm^{-3}) \ w (m s^{-1})	**0.5**	**1**	**2**	**4**	**8**
500	0.33 R^2 = 0.98	0.27 R^2 = 0.92	0.31 R^2 = 0.85	0.32 R^2 = 0.92	-
1000	0.35 R^2 = 0.98	0.32 R^2 = 0.99	0.30 R^2 = 0.95	0.32 R^2 =1.00	0.41 R^2 = 0.94
3000	0.14 R^2 = 0.62	0.23 R^2 = 0.90	0.28 R^2 = 0.96	0.26 R^2 = 0.97	0.27 R^2 = 0.96
4500	0.19 R^2 = 0.95	0.24 R^2 = 0.98	0.24 R^2 = 0.99	0.26 R^2 = 0.97	-

Table S3. sensitivities of D_{eff} to H - $\boldsymbol{S_{D_{eff}}(H) = \frac{\partial lnD_{eff}}{\partial lnH}\Big|_{N_a,w}}$. Intervals upper limits are highlighted in bold letters.

w (m s^{-1}) \ H (m)	**200**	**500**	**950**	**1625**	**2637.5**	**4156.25**
0.5	0.69 R^2 = 0.97	0.75 R^2 = 0.82	1.23 R^2 = 0.89	0.64 R^2 = 0.86	-0.069 R^2 = 0.011	1.24 R^2 = 0.83
1	0.67 R^2 = 0.90	0.79 R^2 = 0.87	0.90 R^2 = 1.00	0.87 R^2 = 0.88	0.70 R^2 = 1.00	1.11 R^2 = 0.95
2	0.72 R^2 = 0.84	0.89 R^2 = 0.98	1.049 R^2 = 0.94	0.87 R^2 = 0.92	0.90 R^2 = 0.92	1.40 R^2 = 0.96
4	0.54 R^2 = 0.62	0.85 R^2 = 0.95	0.79 R^2 = 0.99	0.49 R^2 = 0.37	0.72 R^2 = 0.92	1.22 R^2 = 0.98
8	-	-	-	-	0.94 R^2 = 1.00	0.83 R^2 = 0.98

Table S4. sensitivities of N_d to N_a - $\boldsymbol{S_{N_d}(N_a) = \frac{\partial lnN_d}{\partial lnN_a}\Big|_{w,H}}$. Intervals upper limits are highlighted in bold letters.

N_a (cm^{-3}) \ H (m)	**200**	**500**	**950**	**1625**	**2637.5**	**4156.25**
500	0.57 R^2 = 1.00	0.46 R^2 = 0.89	0.86 R^2 = 0.97	-0.12 R^2 = 0.070	0.40 R^2 = 0.76	-
1000	0.45 R^2 = 0.91	0.44 R^2 = 0.99	0.34 R^2 = 0.47	0.32 R^2 = 0.89	0.29 R^2 = 0.91	0.64 R^2 = 0.89
3000	0.61 R^2 = 0.94	0.85 R^2 = 0.96	-	0.37 R^2 = 0.82	0.39 R^2 = 0.95	0.65 R^2 = 0.92
4500	0.24 R^2 = 0.91	0.30 R^2 = 0.89	0.41 R^2 = 0.67	-0.37 R^2 = 0.46	1.034 R^2 = 0.70	0.38 R^2 = 0.90

Table S5. sensitivities of N_d to w - $\boldsymbol{S_{N_d}(w) = \left.\frac{\partial ln N_d}{\partial ln w}\right|_{N_a,H}}$. Intervals upper limits are highlighted in bold letters.

N_a (cm^{-3}) \ w (m s^{-1})	**0.5**	**1**	**2**	**4**	**8**
500	0.20 R^2 = 0.11	-0.29 R^2 = 0.97	-0.084 R^2 = 0.20	-0.094 R^2 = 0.080	-
1000	-0.24 R^2 = 0.36	-0.21 R^2 = 0.24	-0.22 R^2 = 0.21	-0.26 R^2 = 0.54	-0.15 R^2 = 0.64
3000	-0.11 R^2 = 0.97	-0.14 R^2 = 0.26	-0.22 R^2 = 0.94	-0.32 R^2 = 0.89	-0.26 R^2 = 0.85
4500	-0.26 R^2 = 0.094	0.068 R^2 = 0.14	0.075 R^2 = 0.056	0.081 R^2 = 0.022	-

Table S6. sensitivities of N_d to H - $\boldsymbol{S_{N_d}(H) = \left.\frac{\partial ln N_d}{\partial ln H}\right|_{N_a,w}}$. Intervals upper limits are highlighted in bold letters.

w (m s^{-1}) \ H (m)	**200**	**500**	**950**	**1625**	**2637.5**	**4156.25**
0.5	0.30 R^2 = 0.97	-0.11 R^2 = 0.070	0.48 R^2 = 0.66	-0.022 R^2 = 0.013	-1.11 R^2 = 0.82	0.058 R^2 = 0.0052
1	0.24 R^2 = 0.40	-0.030 R^2 = 0.0072	0.055 R^2 = 0.42	0.43 R^2 = 0.50	0.024 R^2 = 0.12	0.62 R^2 = 0.90
2	0.22 R^2 = 0.26	0.021 R^2 = 0.019	0.23 R^2 = 0.21	0.41 R^2 = 0.34	-0.043 R^2 = 0.097	0.60 R^2 = 0.41
4	0.032 R^2 = 0.0033	-0.025 R^2 = 0.0067	0.015 R^2 = 0.054	-0.42 R^2 = 0.25	-0.12 R^2 = 0.29	0.20 R^2 = 0.98
8	-	-	-	-	0.15 R^2 = 0.17	-0.20 R^2 = 0.90

Table S7. sensitivities of LWC to N_a - $\boldsymbol{S_{LWC}(N_a) = \frac{\partial lnLWC}{\partial lnN_a}\Big|_{w,H}}$. Intervals upper limits are highlighted in bold letters.

N_a (cm^{-3}) \ H (m)	**200**	**500**	**950**	**1625**	**2637.5**	**4156.25**
500	0.62 R^2 = 1.00	0.60 R^2 = 0.85	1.024 R^2 = 0.98	0.060 R^2 = 0.0047	0.34 R^2 = 0.91	-
1000	0.50 R^2 = 0.87	0.42 R^2 = 0.90	0.37 R^2 = 0.43	0.42 R^2 = 0.88	0.31 R^2 = 0.85	0.69 R^2 = 0.75
3000	0.70 R^2 = 0.97	0.94 R^2 = 0.94	-	0.33 R^2 = 0.72	0.70 R^2 = 0.96	0.89 R^2 = 0.87
4500	0.10 R^2 = 0.44	0.33 R^2 = 0.84	0.53 R^2 = 0.70	-0.47 R^2 = 0.64	1.00 R^2 = 0.66	0.42 R^2 = 0.81

Table S8. sensitivities of LWC to w - $\boldsymbol{S_{LWC}(w) = \frac{\partial lnLWC}{\partial lnw}\Big|_{N_a,H}}$. Intervals upper limits are highlighted in bold letters.

N_a (cm^{-3}) \ w (m s^{-1})	**0.5**	**1**	**2**	**4**	**8**
500	1.14 $R^2 = 0.83$	0.27 $R^2 = 0.45$	0.74 $R^2 = 0.62$	0.80 $R^2 = 0.84$	-
1000	0.73 $R^2 = 0.92$	0.69 $R^2 = 0.90$	0.65 $R^2 = 0.65$	0.71 $R^2 = 0.92$	1.062 $R^2 = 0.79$
3000	0.51 $R^2 = 0.61$	0.58 $R^2 = 0.76$	0.64 $R^2 = 0.95$	0.48 $R^2 = 0.92$	0.52 $R^2 = 0.86$
4500	0.36 $R^2 = 0.16$	0.77 $R^2 = 0.98$	0.70 $R^2 = 0.83$	0.76 $R^2 = 0.62$	-

Table S9. sensitivities of LWC to H - $\boldsymbol{S_{LWC}(H) = \frac{\partial lnLWC}{\partial lnH}\Big|_{N_a,w}}$. Intervals upper limits are highlighted in bold letters.

w (m s^{-1}) \ H (m)	**200**	**500**	**950**	**1625**	**2637.5**	**4156.25**
0.5	-0.25 $R^2 = 0.50$	0.20 $R^2 = 0.50$	0.51 $R^2 = 0.70$	0.43 $R^2 = 0.74$	0.53 $R^2 = 0.87$	0.54 $R^2 = 0.40$
1	-0.33 $R^2 = 0.76$	0.12 $R^2 = 0.17$	0.62 $R^2 = 0.87$	0.37 $R^2 = 0.87$	0.37 $R^2 = 62$	0.74 $R^2 = 0.86$
2	-0.42 $R^2 = 0.93$	0.11 $R^2 = 0.28$	0.40 $R^2 = 0.91$	0.40 $R^2 = 0.66$	0.51 $R^2 = 0.86$	0.069 $R^2 = 0.13$
4	-0.54 $R^2 = 0.97$	-0.15 $R^2 = 0.39$	0.062 $R^2 = 0.20$	0.29 $R^2 = 0.36$	0.56 $R^2 = 0.88$	0.14 $R^2 = 0.18$
8	-	-	-	-	0.52 $R^2 = 0.99$	0.090 $R^2 = 0.93$

Table S10. sensitivities of Λ to N_a - $\boldsymbol{S_{\Lambda}(N_a) = \frac{\partial ln\Lambda}{\partial lnN_a}\Big|_{w,H}}$. Intervals upper limits are highlighted in bold letters.

N_a (cm^{-3}) \ H (m)	**200**	**500**	**950**	**1625**	**2637.5**	**4156.25**
500	0.35 R^2 =0.98	0.35 R^2 = 0.65	0.41 R^2 = 0.66	0.049 R^2 = 0.14	-0.090 R^2 = 0.98	-
1000	0.061 R^2 = 0.24	0.0043 R^2 = 0.0037	-0.062 R^2 = 0.11	0.19 R^2 = 0.67	-0.11 R^2 = 0.75	0.24 R^2 = 0.82
3000	-0.062 R^2 = 0.31	0.13 R^2 = 0.55	-	0.015 R^2 = 0.045	-0.14 R^2 = 0.83	-0.15 R^2 = 0.42
4500	-0.0064 R^2 = 0.13	-0.11 R^2 = 0.91	-0.097 R^2 = 0.82	-0.18 R^2 = 0.23	0.0068 R^2 = 0.0089	0.049 R^2 = 0.56

Table S11. sensitivities of Λ to w - $\boldsymbol{S_\Lambda(w) = \left.\frac{\partial ln\Lambda}{\partial lnw}\right|_{N_a,H}}$. Intervals upper limits are highlighted in bold letters.

N_a (cm^{-3}) \ w (m s^{-1})	**0.5**	**1**	**2**	**4**	**8**
500	-0.75 R^2 = 0.96	-0.84 R^2 = 0.94	-0.94 R^2 = 0.98	-1.11 R^2 = 0.97	-
1000	-0.61 R^2 = 0.98	-0.63 R^2 = 0.96	-0.47 R^2 = 0.87	-0.54 R^2 = 0.86	-0.25 R^2 = 0.073
3000	-0.10 R^2 = 0.088	-0.17 R^2 = 0.48	-0.25 R^2 = 0.54	-0.21 R^2 = 0.34	-0.26 R^2 = 0.38
4500	-0.17 R^2 = 0.47	-0.15 R^2 = 0.43	-0.15 R^2 = 0.50	-0.14 R^2 = 0.62	-

Table S12. sensitivities of Λ to H - $\boldsymbol{S_\Lambda(H) = \left.\frac{\partial ln\Lambda}{\partial lnH}\right|_{N_a,w}}$. Intervals upper limits are highlighted in bold letters.

w (m s^{-1}) \ H (m)	**200**	**500**	**950**	**1625**	**2637.5**	**4156.25**
0.5	0.17 R^2 = 0.81	0.013 R^2 = 0.014	-0.17 R^2 = 0.45	-0.12 R^2 = 0.66	-0.097 R^2 = 0.56	-0.097 R^2 = 0.36
1	0.21 R^2 = 0.93	0.066 R^2 = 0.21	-0.19 R^2 = 0.75	-0.11 R^2 = 0.80	-0.080 R^2 = 38	-0.24 R^2 = 0.77
2	0.30 R^2 = 0.95	0.027 R^2 = 0.068	-0.12 R^2 = 0.98	-0.14 R^2 = 0.50	-0.14 R^2 = 0.72	0.036 R^2 = 0.090
4	0.44 R^2 = 1.00	0.091 R^2 = 0.24	0.0092 R^2 = 0.018	-0.072 R^2 = 0.12	-0.17 R^2 = 0.70	0.0031 R^2 = 0.0012
8	-	-	-	-	-0.18 R^2 = 0.94	0.16 R^2 = 0.95

Table S13. sensitivities of ε to N_a - $\boldsymbol{S_\varepsilon(N_a)} = \left.\frac{\partial ln\varepsilon}{\partial ln N_a}\right|_{w,H}$. Intervals upper limits are highlighted in bold letters.

N_a (cm^{-3}) \ H (m)	**200**	**500**	**950**	**1625**	**2637.5**	**4156.25**
500	-0.29 R^2 =0.95	-0.11 R^2 = 0.60	-0.19 R^2 = 0.80	0.015 R^2 = 0.057	0.063 R^2 = 1.00	-
1000	-0.080 R^2 = 0.41	-0.016 R^2 = 0.71	0.076 R^2 = 0.34	-0.12 R^2 = 0.78	0.049 R^2 = 0.53	-0.14 R^2 = 0.86
3000	0.037 R^2 = 0.31	-0.17 R^2 = 0.76	-	0.00013 R^2 = 0.000024	0.0024 R^2 = 0.0019	-0.035 R^2 = 0.22
4500	0.027 R^2 = 0.51	0.037 R^2 = 0.61	0.024 R^2 = 0.53	0.018 R^2 = 0.30	-0.025 R^2 = 0.27	-0.023 R^2 = 0.28

Table S14. sensitivities of ε to w - $\boldsymbol{S_\varepsilon(w)} = \left.\frac{\partial ln\varepsilon}{\partial ln w}\right|_{N_a,H}$. Intervals upper limits are highlighted in bold letters.

N_a (cm^{-3}) \ w (m s^{-1})	**0.5**	**1**	**2**	**4**	**8**
500	0.22 R^2 = 0.85	0.30 R^2 = 0.73	0.36 R^2 = 0.94	0.48 R^2 = 0.99	-
1000	0.15 R^2 = 0.79	0.16 R^2 = 0.82	0.094 R^2 = 0.63	0.16 R^2 = 0.74	-0.16 R^2 = 0.084
3000	0.0066 R^2 = 0.0045	0.0093 R^2 = 0.030	0.017 R^2 = 0.046	0.028 R^2 = 0.032	0.010 R^2 = 0.0024
4500	-0.022 R^2 = 0.062	-0.037 R^2 = 0.20	-0.036 R^2 = 0.17	-0.046 R^2 = 0.29	-

Table S15. sensitivities of ε to H - $\boldsymbol{S_{\varepsilon}(H) = \frac{\partial ln\varepsilon}{\partial lnH}\Big|_{N_a,w}}$. Intervals upper limits are highlighted in bold letters.

w (m s^{-1}) \ H (m)	**200**	**500**	**950**	**1625**	**2637.5**	**4156.25**
0.5	289	89	21	32	36	45
1	247	82	20	24	22	45
2	223	87	26	34	28	49
4	111	47	30	37	29	38
8	0	0	0	0	18	27

Table S16. number of 1 Hz DSD data for the sensitivities to N_a.

N_a (cm^{-3}) \ H (m)	**200**	**500**	**950**	**1625**	**2637.5**	**4156.25**
500	259	84	28	27	11	0
1000	234	84	38	40	56	81
3000	265	91	0	61	43	75
4500	125	55	25	16	23	44

Table S17. number of 1 Hz DSD data for the sensitivities to w.

N_a (cm^{-3}) \ w (m s^{-1})	**0.5**	**1**	**2**	**4**	**8**
500	169	119	90	35	0
1000	137	136	146	94	20
3000	142	100	138	110	51
4500	64	85	73	53	0

Table S18. number of 1 Hz DSD data for the sensitivities to H.